Nitric Oxide Increases Cardiac I_{K1} by Nitrosylation of Cysteine 76 of Kir2.1 Channels

Ricardo Gómez,* Ricardo Caballero,* Adriana Barana, Irene Amorós, Enrique Calvo, Juan Antonio López, Helene Klein, Miguel Vaquero, Lourdes Osuna, Felipe Atienza, Jesús Almendral, Ángel Pinto, Juan Tamargo, Eva Delpón

Rationale: The cardiac inwardly rectifying K^+ current (I_{K1}) plays a critical role in modulating excitability by setting the resting membrane potential and shaping phase 3 of the cardiac action potential.

Objective: This study aims to analyze the effects of nitric oxide (NO) on human atrial I_{K1} and on Kir2.1 channels, the major isoform of inwardly rectifying channels present in the human heart.

Methods and Results: Currents were recorded in enzymatically isolated myocytes and in transiently transfected CHO cells, respectively. NO at myocardial physiological concentrations (25 to 500 nmol/L) increased inward and outward I_{K1} and $I_{Kir2.1}$. These effects were accompanied by hyperpolarization of the resting membrane potential and a shortening of the duration of phase 3 of the human atrial action potential. The $I_{Kir2.1}$ increase was attributable to an increase in the open probability of the channel. Site-directed mutagenesis analysis demonstrated that NO effects were mediated by the selective *S*-nitrosylation of Kir2.1 Cys76 residue. Single ion monitoring experiments performed by liquid chromatography/tandem mass spectrometry suggested that the primary sequence that surrounds Cys76 determines its selective *S*-nitrosylation. Chronic atrial fibrillation, which produces a decrease in NO bioavailability, decreased the *S*-nitrosylation of Kir2.1 channels in human atrial samples as demonstrated by a biotin-switch assay, followed by Western blot.

Conclusions: The results demonstrated that, under physiological conditions, NO regulates human cardiac I_{K1} through a redox-related process. (*Circ Res*. 2009;105:383-392.)

Key Words: nitric oxide ■ Kir2.1 channels ■ resting membrane potential ■ cardiac myocytes ■ I_{K1}

The hallmark of the cardiac inwardly rectifying K^+ current (I_{K1}) is the strong inward rectification; that is, the preferential conduction of inward compared to outward current.[1] I_{K1} provides a large inward conductance at membrane potentials below the reversal potential of K^+ (E_K), and a relatively large outward conductance at potentials just above E_K, which helps to maintain the resting membrane potential (RMP) close to E_K and controls the approach to threshold on depolarization. In contrast, I_{K1} channels remain closed throughout the plateau phase of the cardiac action potential (AP), which permits relatively small inward currents to maintain the plateau. Thereafter, on repolarization (at potentials negative to −20 mV), I_{K1} provides substantial K^+ efflux to contribute to phase 3 of repolarization.[2] Therefore, I_{K1} plays a critical role in modulating cardiac excitability by setting the diastolic RMP and shaping the initial depolarization and the final repolarization phases of the AP in both atria and ventricles.[2]

In the human heart, 3 inwardly rectifying channels (Kir2.1, Kir2.2, and Kir2.3) contribute to I_{K1}.[3] Experimental data suggest that the Kir2.1 channel is the major isoform underlying ventricular I_{K1}, whereas its relative contribution to atrial I_{K1} seems to be lower.[4] In fact, gain- and loss-of-function mutations in the gene encoding Kir2.1 (KCNJ2) have been reported to cause short QT and long QT (Andersen–Tawil) syndromes, respectively.[5] Both syndromes, particularly the former, are associated with severe ventricular arrhythmias. Indeed, the importance of I_{K1} in the establishment of a fast and stable reentry of spiral waves (rotors) and ventricular fibrillation dynamics has been demonstrated.[6]

Nitric oxide (NO) is a gaseous mediator produced by all myocardial cell types. In the heart, NO plays an important role in regulating rate, contractile function, coronary tone, myocardial oxygen consumption, mitochondrial respiration, autonomic signaling, and cell growth and survival.[7] Using conventional microelectrode techniques, we recently de-

Original received November 7, 2008; resubmission received March 19, 2009; revised resubmission received July 1, 2009; accepted July 2, 2009.

From the Department of Pharmacology (R.G., R.C., A.B., I.A., M.V., L.O., J.T., E.D.), School of Medicine, Universidad Complutense, Madrid, Spain; Centro Nacional de Investigaciones Cardiovasculares (E.C., J.A.L.), Madrid, Spain; Department of Physiology, Montreal University (H.K.), Canada; and Hospital General Universitario Gregorio Marañón (F.A., J.A., A.P.), Madrid, Spain.

*Both authors contributed equally to this work.

Correspondence to Ricardo Caballero, Department of Pharmacology, School of Medicine, Universidad Complutense, 28040 Madrid, Spain. E-mail rcaballero@med.ucm.es

Circulation Research is available at http://circres.ahajournals.org DOI: 10.1161/CIRCRESAHA.109.197558

Non-standard Abbreviations and Acronyms

τ_o	open-time constant
τ_c	closed-time constant
AP	action potential
APD	action potential duration
cAF	chronic atrial fibrillation
CHO	Chinese hamster ovary cells
DEANO	*N,N*-diethylamine-diazenolate-2-oxide
DTT	dithiothreitol
E_K	reversal potential of K^+
f_o	opening frequency
I_{K1}	cardiac inwardly rectifying K^+ current
I_{KACh}	acetylcholine-activated component of the inward rectifier current
I_{KATP}	ATP-sensitive K^+ current
$I_{Kir2.1}$	Kir2.1 current
Kir2.1Cyt	peptide of the Kir2.1 cytoplasmic region spanning residues 48 to 80
I_{NCX}	Na^+/Ca^{2+} exchange current
I-V	current–voltage
$[K^+]_o$	extracellular K^+ concentration
LC-MS	liquid chromatography/tandem mass spectrometry
NO	nitric oxide
ODQ	1*H*-[1,2,4]oxadiazolo[4,3-a]quinoxalin-1-one
P_o	open probability
RMP	resting membrane potential
sGC	soluble guanylyl cyclase
SIM	single ion monitoring
SNAP	(±)-*S*-nitroso-*N*-acetylpenicillamine
SR	sinus rhythm
WT	wild type

scribed that NO, at physiological myocardial concentrations, hyperpolarizes RMP and shortens AP duration (APD) measured at 50% and 90% of repolarization in mouse isolated atria.[8] NO-induced shortening appeared in the range of membrane potentials negative to −40 mV, which corresponds to the phase of repolarization where the contribution of I_{K1} is most significant, suggesting that NO regulates I_{K1}.

Thus, in this study, the effects of NO on human atrial I_{K1} and Kir2.1 channels, as well as the mechanisms involved in these actions, have been analyzed. The results demonstrated that NO regulates cardiac excitability by the selective *S*-nitrosylation of Cys76 of the Kir2.1 protein.

Methods

The study was approved by the Investigation Committee of the Hospital Universitario Gregorio Marañón (CNIC-13) and conforms to the principles outlined in the Declaration of Helsinki. Each patient gave written informed consent. Myocytes were enzymatically isolated from right atrial appendages obtained from patients in sinus rhythm (SR) undergoing cardiac surgery.[8]

Human Kir2.1 wild-type (WT) and mutated channels were transiently transfected in CHO cells.[8,9] The NO donors (±)-*S*-nitroso-*N*-acetylpenicillamine (SNAP) and *N,N*-diethylamine-diazenolate-2-oxide (DEANO) were initially dissolved in ethanol and water, respectively and the NO-saturated solution was obtained as described.[8,9] Macroscopic and single-channel currents were recorded using the whole-cell and cell-attached patch-clamp configurations, respectively.

The *S*-nitrosylation of a synthetic peptide spanning sequence 48-VKKDGHCNVQFINVGEKGQRYLADIFTTCVDIR-80 from the cytoplasmic tail of Kir2.1 was determined by liquid chromatography/tandem mass spectrometry (LC-MS). Single ion monitoring (SIM) experiments were performed for the masses corresponding to the unmodified and nitrosylated-tryptic peptides. Detection of *S*-nitrosylated Kir2.1 in mouse ventricular and human atrial samples was performed using the biotin-switch assay, followed by Western blot.[8,9]

Results are expressed as mean±SEM. Paired or unpaired *t* test or 1-way ANOVA followed by Newman–Keuls test were used to assess statistical significance where appropriate. A value of $P<0.05$ was considered significant.

An expanded Methods section is available in the Online Data Supplement at http://circres.ahajournals.org.

Results

NO Increases Human Atrial I_{K1}

Figure 1 shows original recordings (Figure 1A) and mean current–voltage (I-V) relationships (Figure 1B) for I_{K1} obtained in isolated human atrial myocytes by applying a voltage ramp from −100 to −10 mV in the absence and presence of the NO donor SNAP (200 μmol/L). SNAP increased both inward (23.6±5.5% at −100 mV) and outward I_{K1} (67.9±12.4% at −10 mV) (n=8, $P<0.05$ versus control). These experiments were performed in the presence of atropine (1 μmol/L) to block the acetylcholine-activated component of the inward rectifier current (I_{KACh}). Under these conditions, activation of the ATP-sensitive K^+ current (I_{KATP}) is very unlikely because intracellular solution was supplemented with ATP. Nevertheless, we analyzed the effects of SNAP in the presence of glibenclamide (10 μmol/L), a selective I_{KATP} blocker. Figure 1E demonstrates that even in the presence of glibenclamide, SNAP increased the I_{K1} measured at −100 mV by 18.2±2.8% (n=4, $P<0.05$). To further isolate the effects of SNAP on I_{K1}, we used $BaCl_2$ (100 μmol/L), a selective blocker of I_{K1} in the presence of atropine and glibenclamide. Application of SNAP increased the Ba^{2+}-sensitive current, which displayed strong inward rectification, without modifying the Ba^{2+}-insensitive current, adding strong support to the hypothesis that the current increased by SNAP is I_{K1} (Figure 1C and 1E). However, as can be observed in the inset of Figure 1C the SNAP-increased Ba^{2+}-sensitive current seemed to display less inward rectification than I_{K1}. Moreover, the Na^+/Ca^{2+} exchange current (I_{NCX}) can also be activated over the voltage range tested. Therefore we analyzed the effects of SNAP on I_{NCX}. Extracellular solution (containing atropine and glibenclamide) was supplemented with ouabain (10 μmol/L) to inhibit the Na^+/K^+ ATPase and I_{NCX} was measured as the difference between the current recorded in the presence of extracellular Ca^{2+} and that recorded in the presence of 5 mmol/L Ni^{2+} (0 mmol/L Ca^{2+}). Online Figure I demonstrates that SNAP did not modify the I_{NCX}.

Next, the effects of SNAP on APs recorded in isolated human atrial myocytes were analyzed. As shown in Figure 1D, application of SNAP (in the presence of atropine and glibenclamide) slightly but significantly hyperpolarized the RMP (from −69.8±2.7 to −72.8±3.2 mV, n=4, $P<0.05$)

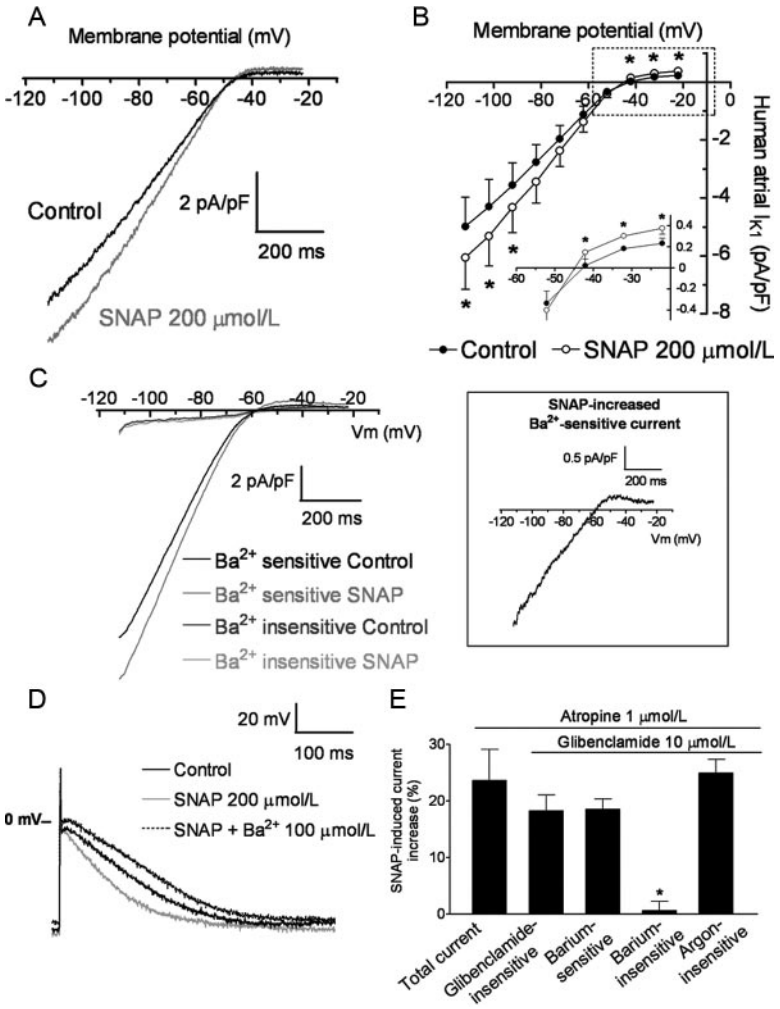

Figure 1. SNAP increases human atrial I_{K1}. A, Voltage ramp (800 ms) from −100 to −10 mV in the absence and presence of 200 μmol/L SNAP. B, I-V curves for human atrial I_{K1} in the absence and presence of SNAP. The inset shows data at potentials positive to E_K in an expanded scale. C, Representative Ba^{2+}-sensitive and Ba^{2+}-insensitive currents recorded before and after application of SNAP by applying a voltage ramp (800 ms) from −100 to −10 mV. The inset (right box) shows the SNAP-increased Ba^{2+}-sensitive current. In panels A to C, the voltage is adjusted to the liquid junction potential of 12.1 mV. D, AP recorded in a human atrial myocyte in control conditions (1 μmol/L atropine and 10 μmol/L glibenclamide), in the presence of SNAP and after perfusion of SNAP and Ba^{2+}. E, Percentage of I_{K1} SNAP-induced increase at −100 mV under different experimental conditions. Each point/column represents the mean±SEM of ≥4 experiments. *$P<0.05$ vs control.

and shortened the APD_{90} (from 227±12 to 173±16 ms, $P<0.05$). Further addition of Ba^{2+} not only completely reversed the effect of SNAP but also increased the APD_{90} to 286±46 ms and depolarized the RMP (−64.9±1.3 mV, $P<0.05$). These results suggest that the NO effects on I_{K1} have a significant impact on the shape of human atrial AP.

NO Increases Kir2.1 Currents

Because human I_{K1} is mainly carried by Kir2.1 channels, we studied the effects of NO on Kir2.1 currents ($I_{Kir2.1}$) recorded in transiently transfected CHO cells. Figure 2A shows $I_{Kir2.1}$ recorded by applying 250-ms pulses from −60 mV to potentials ranging −120 and +20 mV in the absence and presence of 200 μmol/L SNAP. SNAP increased $I_{Kir2.1}$ at voltages negative (20.9±5.9% at −120 mV) and positive to E_K (51.7±11.1% at −50 mV) (Figure 2A and 2B) (n=7, $P<0.05$). The SNAP-induced increase was completely reversible on washout. The time course of the NO concentrations in the cell chamber after beginning the SNAP perfusion was measured using a potentiometric NO sensor (see Online Data Supplement).[8,9] NO concentration reached a maximum within 4 to 6 minutes (182±35 nmol/L with SNAP 200 μmol/L, n=7) and remained stable during SNAP perfusion (10 to 12 minutes), decreasing to basal levels after perfusion with SNAP-free solution. In Figure 2C, the $I_{Kir2.1}$ increase measured at the end of pulses to −120 mV was represented as a function of the SNAP concentration. At concentrations higher than 200 μmol/L SNAP induced a similar amount of increase. The Hill equation was used to fit the concentration dependence of the increase, and the EC_{50} and the maximum effect obtained were 82.8±3.6 μmol/L (n_H=3.1±0.8) and 21.5±0.5%, respectively. When the increase was plotted as a function of the released NO, the EC_{50} was 75.4±3.4 nmol/L (n_H=3.1±0.8) (Figure 2D).

The effects of another NO donor (3 μmol/L DEANO) and an NO-saturated solution, which yielded NO concentrations of 247±23 and 205±13 nmol/L, respectively (Figure 3A and 3B), were also studied. To prepare the NO-saturated solution, the external solution was bubbled with argon (Ar) for 20 to 30 minutes in a gas-washing bottle obtaining an O_2-free solution and, then, with NO for 30 minutes (see Online Data Supplement). Control data were obtained in the presence of the O_2-free Ar-saturated solution.[8,9] DEANO (Figure 3C) and the NO solution (Figure 3D) also significantly increased inward $I_{Kir2.1}$ by 17.3±2.5% (n=7) and 17.7±1.4% (n=4) at −120 mV, respectively, and outward $I_{Kir2.1}$ by 52.3±12.0% and 60.3±2.2% at −50 mV, respectively. These effects were not different from those obtained with SNAP at concentrations that release equivalent levels of NO and indicated that, in all cases, the $I_{Kir2.1}$ increase was exclusively attributable to NO.

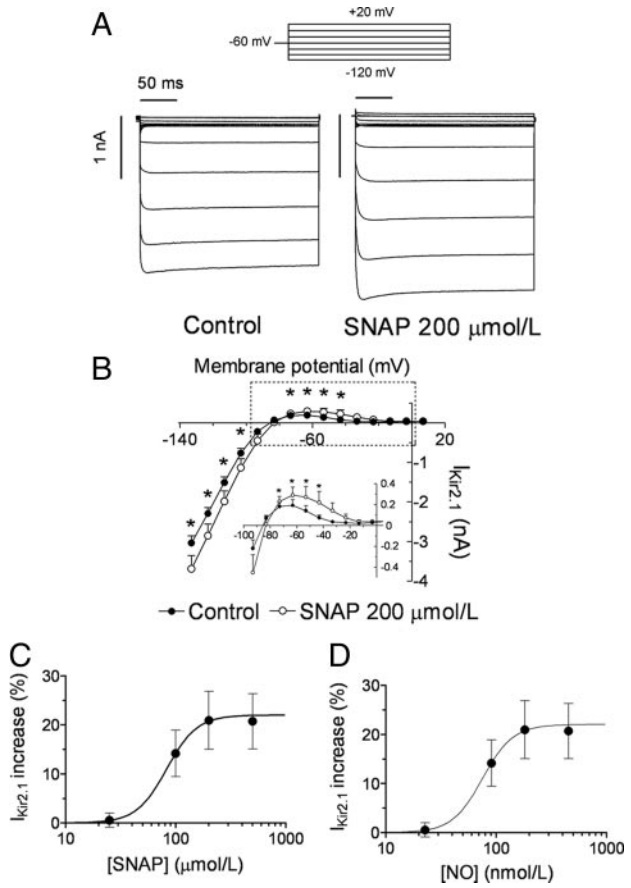

Figure 2. SNAP increases $I_{Kir2.1}$. A, $I_{Kir2.1}$ traces recorded by applying 250-ms pulses from a holding potential of −60 mV to potentials ranging −120 and +20 mV in the absence and presence of 200 μmol/L SNAP. B, I-V curves for currents measured at the end of the pulses. The inset shows data at potentials positive to E_K in an expanded scale. Percentage of $I_{Kir2.1}$ increase at −120 mV as a function of SNAP (C) and the released NO (D) concentrations. Each point represents the mean±SEM of >7 experiments. *P<0.05 vs control.

Because it has been demonstrated that hypoxia increases mouse cardiac I_{K1},[10] we analyzed the effects of SNAP when added to an O_2-free Ar-saturated solution on human atrial I_{K1}. Control data were obtained in the presence of an O_2-free Ar-saturated solution. Figure 1E shows that SNAP increased the Ar-insensitive current at −100 mV by 24.9±2.4% (P<0.05, n=4). Therefore, increasing effects produced by NO were apparent even in hypoxic conditions.

NO-Induced Increase Is Not Dependent on the Extracellular K^+ Concentration

Kir2.1 channel conductance and inward rectification are strongly dependent on the extracellular K^+ concentration ($[K^+]_o$).[1,2] Therefore, we analyzed whether the NO-induced increase was dependent on the $[K^+]_o$, by comparing the effects of SNAP on $I_{Kir2.1}$ recorded at 1 and 10 mmol/L $[K^+]_o$ (Figure 4) with those observed at 4 mmol/L. Progressive increase of $[K^+]_o$ produced an increase in inward and outward $I_{Kir2.1}$ and a rightward shift in the E_K (Figure 4A). Figure 4C and 4D shows I-V curves in the absence and presence of SNAP at 1 and 10 mmol/L $[K^+]_o$, respectively. At 1 mmol/L $[K^+]_o$, $I_{Kir2.1}$ was recorded by applying 250-ms pulses from −60 mV to potentials ranging −150 and −10 mV, because at this $[K^+]_o$, the E_K was shifted to −127.9±1.3 mV. SNAP increased both inward and outward currents by 22.2±2.6% and 46.4±7.8% at −150 mV and −80 mV, respectively (n=7). At 10 mmol/L (E_K=−68.1±2.6 mV), currents were recorded by applying 250-ms pulses from −60 mV to potentials ranging from −120 to +20 mV, and SNAP also increased $I_{Kir2.1}$ at potentials negative (20.0±7.1% at −100 mV) and positive (59.9±7.9% at −30 mV) to the E_K (n=5). Finally, as shown in Figure 4B, SNAP did not modify the E_K at any of the $[K^+]_o$ tested.

NO Increases Open Probability of Kir2.1 Channels

The effects of NO on unitary Kir2.1 currents were also analyzed. Figure 5A shows single-channel recordings in a CHO cell expressing Kir2.1 channels by applying 1-second pulses to −80 mV from a holding potential of 0 mV in the absence and presence of 200 μmol/L SNAP. Kir2.1 channel activity was characterized by few and long events leading to a mean open probability (P_o) of 0.18±0.01 and an opening frequency (f_o) of 2.6±0.1 Hz (Figure 5D and 5E) (n=6). Amplitude of unitary currents in control conditions and in the presence of 200 μmol/L SNAP were calculated for each experiment from a Gaussian distribution fit to amplitude histograms that were constructed by plotting amplitude data as a function of the number of events per bin (Online Figure II). SNAP did not modify unitary current amplitude (Figure 5F) but induced a significant change in channel gating characterized by a marked increase in the frequency of events, which appeared as brief channel openings (Figure 5A). Open- and closed-time constants (τ_o and τ_c) were calculated for each experiment from the Gaussian distribution fit to dwell-time histograms that were constructed by plotting dwell-time data as a function of the number of events per bin. Figure 5B and C show dwell-time histograms constructed from pooled experiments. SNAP decreased τ_o from 49.4±16.5 to 27.0±3.9 ms and τ_c from 275.5±47.5 to 154.1±64.8 ms (P<0.05) and increased the f_o (6.9±0.2 Hz; P<0.01) (Figure 5E), which eventually led to an increase in the P_o (0.26±0.01; P<0.05) (Figure 5D).

Cys76 Is Responsible for the NO-Induced Increase of Kir2.1

The next step was to elucidate the signaling pathway responsible for the NO-induced $I_{Kir2.1}$ increase. The activation of soluble guanylyl cyclase (sGC)/cGMP/protein kinase G signaling pathway is the most common mechanism implicated in NO effects.[7] For testing whether this pathway was responsible for the effects, 1*H*-[1,2,4]oxadiazolo[4,3-a]quinoxalin-1-one (ODQ), a selective inhibitor of sGC was used. In the presence of ODQ (50 μmol/L), SNAP (200 μmol/L) increased $I_{Kir2.1}$ to a similar extent (19.2±6.9% at −120 mV) as that produced by SNAP alone (n=6, P>0.05), which discards the involvement of the sGC/cGMP/protein kinase G pathway in the effects.

Posttranslational modifications induced by NO have emerged as important mechanisms by which NO can regulate protein function. These modifications include Cys

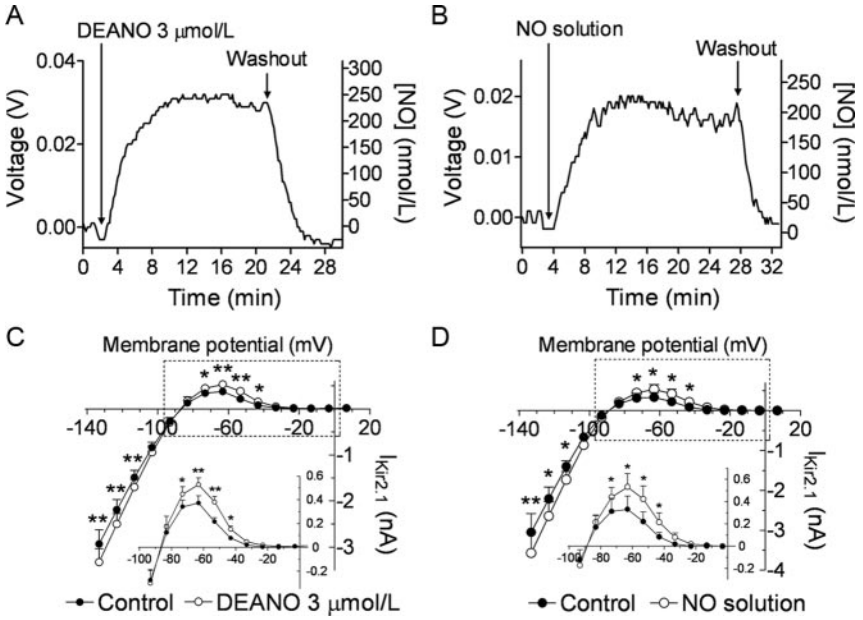

Figure 3. DEANO and an NO solution also increase $I_{Kir2.1}$. NO concentrations yielded before and after perfusion of 3 μmol/L DEANO (A) and an NO-saturated solution (B). I-V curves under control conditions and in the presence of DEANO (C) or the NO solution (D). The insets show data at potentials positive to E_K in an expanded scale. $^*P<0.05$ and $^{**}P<0.01$ vs control. Each point represents the mean±SEM of >4 experiments.

S-nitrosylation and Tyr nitration, which are highly dependent on the cellular redox state.[11] To determine whether some of these modifications could be responsible for the NO-induced increase of $I_{Kir2.1}$, the effects of SNAP in the presence of the reducing agent dithiothreitol (DTT) (5 mmol/L) were studied. DTT per se did not modify $I_{Kir2.1}$ (Figure 6A) but completely prevented the increase induced by SNAP. Identical results were obtained on human atrial I_{K1} (Figure 6B). These results suggested the implication of posttranslational modifications in the effects of NO on $I_{Kir2.1}$ and I_{K1}. The reversibility of the NO-induced increase was in concordance with the characteristic lability of the *S*-nitrosylation of Cys residues, suggesting that this modification was mediating the effects of NO on Kir2.1 channels. To determine the involvement of 1 or some of the 13 Cys of the Kir2.1 channel, site-directed mutagenesis experiments were performed. First, we tried to evaluate the effects of SNAP on a Kir2.1 channel in which all the Cys (with the exception of Cys122 and Cys154, which are essential for proper channel folding),[12] were substituted. However, this "Cys-free" mutant did not generate functional channels. Next, we analyzed the effects of SNAP on IRK1J, a Kir2.1 channel in which 6 Cys residues (C54V, C76V, C89I, C101L, C149F, and C169V) were mutated simultaneously.[13] In IRK1J channels, SNAP failed to modify the current, indicating the implication of 1 or some of these Cys in the NO-induced increase (Figure 6C). To determine which of these Cys was involved, the effects of SNAP on Kir2.1 channels with individual mutations were studied. When possible, substitution of Cys by Ser was chosen because the replacement of Cys-sulfur by the Ser-oxygen keeps the hydrogen bonding capability in most of the cases and, thus, the essential features of the channel (C54S, C101S, C149S).[12] Other substitutions were introduced in those channels in which Ser substitution induced dramatic changes in channel properties (C76L, C76V, C89G, C169A).[12] The characteristics of the currents generated by all these mutants were

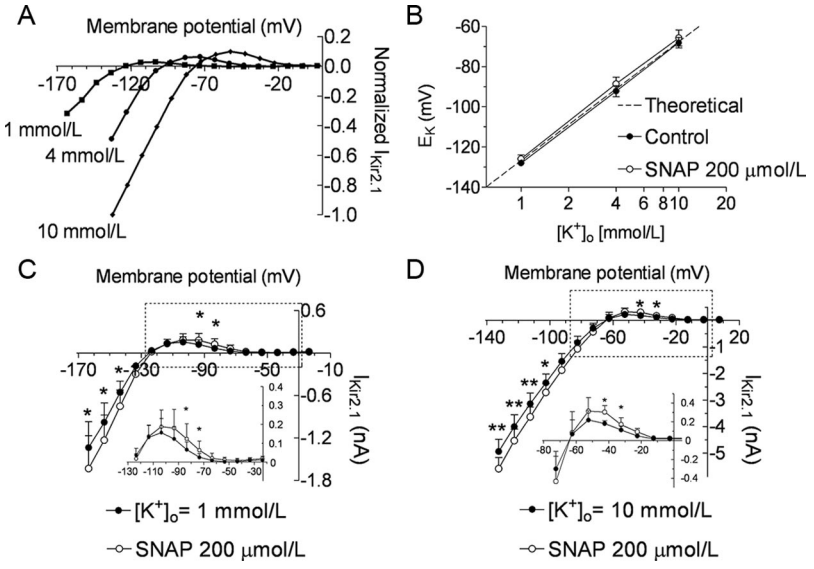

Figure 4. NO-induced increase of $I_{Kir2.1}$ is not dependent on $[K^+]_o$. A, Normalized I-V curves for $I_{Kir2.1}$ recorded in CHO cells perfused with an external solution containing 1, 4, or 10 mmol/L $[K^+]_o$. B, E_K values in the absence and presence of 200 μmol/L SNAP and the theoretical values obtained from the Nernst equation plotted as a function of the $[K^+]_o$. I-V curves under control conditions and in the presence of SNAP at 1 mmol/L (C) or 10 mmol/L $[K^+]_o$ (D). The insets show data at potentials positive to E_K in an expanded scale. $^*P<0.05$ and $^{**}P<0.01$ vs control. Each point represents the mean±SEM of >5 experiments.

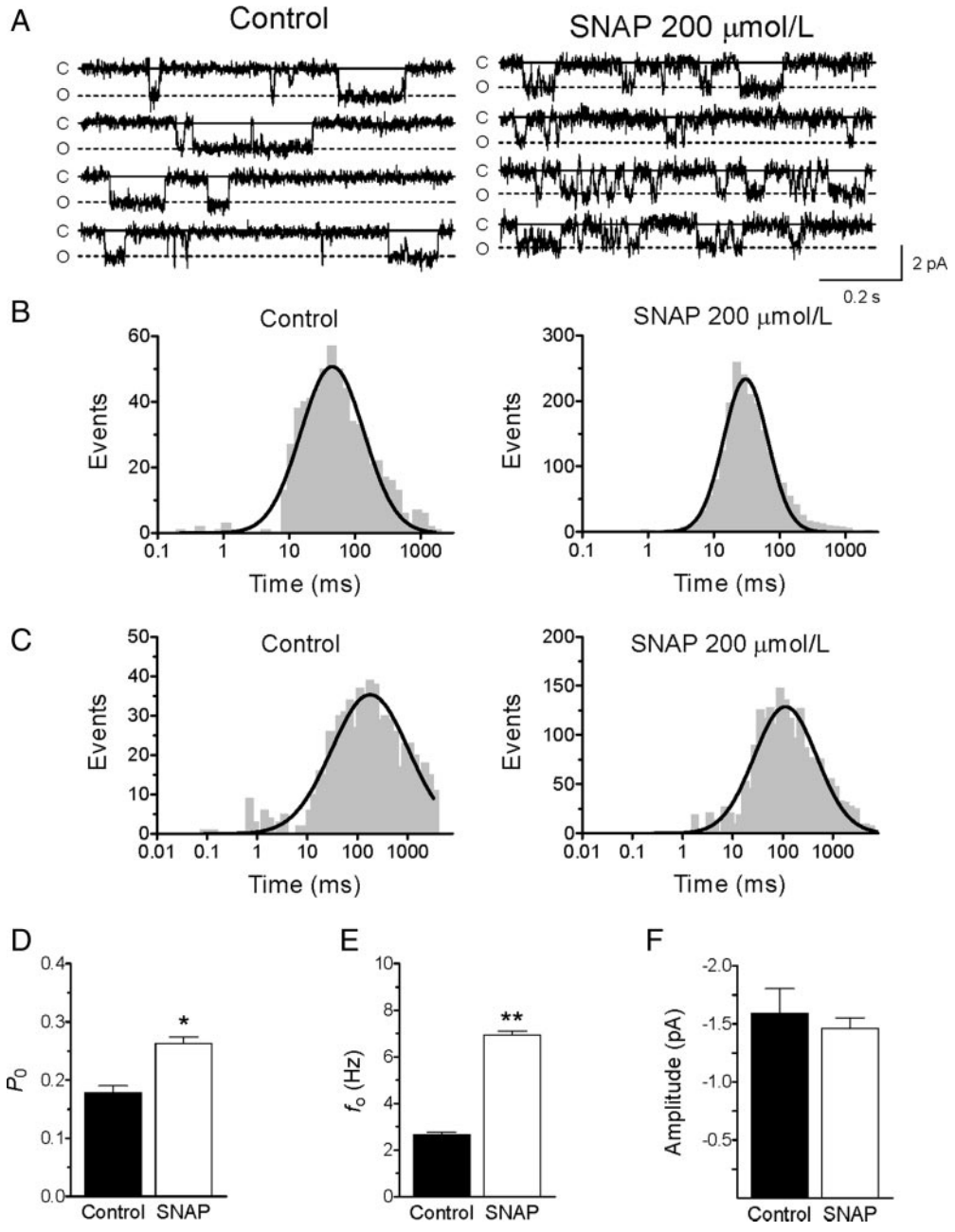

Figure 5. NO increases P_o and f_o but decreases τ_o of Kir2.1 channels. A, Single-channel recordings in a CHO cell under control conditions and after perfusion with 200 μmol/L SNAP. Closed and open channel levels are indicated by C and O, respectively. Dwell-time histograms of open (B) and closed (C) times of single Kir2.1 channels recorded in the absence and presence of SNAP (10 bins/decade). Continuous lines represent the fit of a Gaussian distribution to the data. Histograms were obtained by pooling data from 6 experiments. P_o (D), f_o (E), and unitary current amplitude (F) in the absence and presence of SNAP. Each column represents the mean±SEM of 6 experiments. *$P<0.05$ and **$P<0.01$ vs control.

similar to those of the Kir2.1 WT. SNAP also increased inward and outward currents generated by the mutants, with the exception of C76L and C76V channels, in which SNAP failed to increase $I_{Kir2.1}$ both at potentials negative and positive to E_K (Figure 6D and 6E). The percentage of change at −120 mV for all the constructs is summarized in Figure 6E. These results indicated that Cys76 is critical for the $I_{Kir2.1}$ increase induced by NO. Finally, we studied the effects of SNAP on cells cotransfected with both WT and C76L Kir2.1 channels. Under these conditions, the NO donor failed to increase inward and outward $I_{Kir2.1}$ (Figure 6E).

Residue Cys76 Is Nitrosylated in a Kir2.1 Cytoplasmic Peptide

The thiol group of Cys76 is located in the vicinity of acid and basic residues that could act as catalysts for *S*-nitrosylation.[11] For testing whether the primary sequence of the protein determines the specific *S*-nitrosylation of Cys76, a peptide of the Kir2.1 cytoplasmic region spanning residues 48 to 80 (Kir2.1Cyt), which contained Cys54 and Cys76, was synthesized (Figure 7A). Kir2.1Cyt was treated with SNAP and then trypsin-digested to yield 2 peptides (DGHCNVQFINVGEK and YLADIFTTCVDIR) containing the Cys54 and Cys76

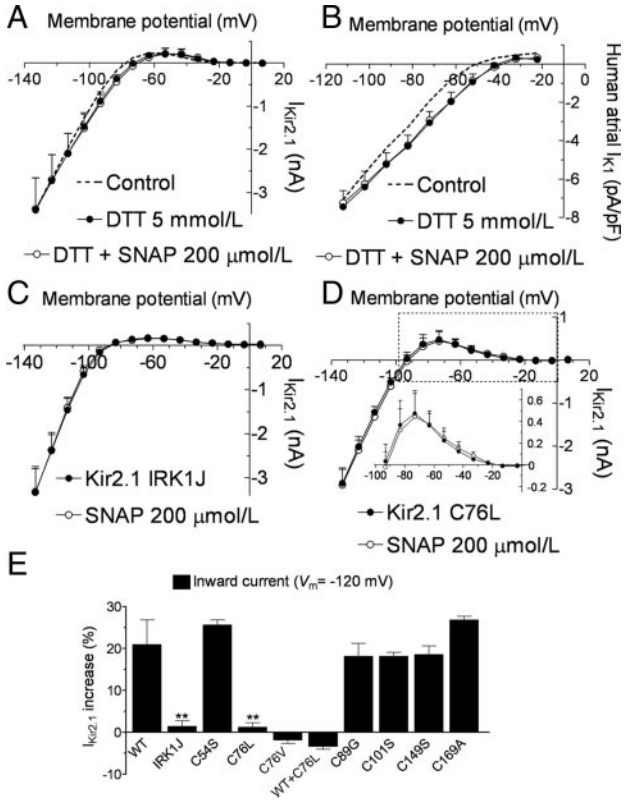

Figure 6. NO-induced increase is dependent on the cellular redox state and is determined by Cys76. I-V curves for $I_{Kir2.1}$ (A) and human atrial I_{K1} (B) in the absence (control, dashed line) and presence of DTT (5 mmol/L) alone or plus SNAP (200 μmol/L). I-V curves for currents recorded in CHO cells expressing IRK1J (C) or C76L (D) Kir2.1 channels in the absence and presence of SNAP. E, SNAP-induced change on the current recorded at −120 mV in CHO cells expressing WT or mutant Kir2.1 channels. $^{**}P<0.01$ vs WT. Each point/column represents the mean±SEM of >4 experiments.

residues, respectively. SIM experiments were performed by LC-MS for masses at *m/z* 780.3 and 794.8 Da (unmodified and nitrosylated Cys54, respectively), and at *m/z* 765.3 and 779.8 Da (unmodified and nitrosylated Cys76, respectively), corresponding to doubly charged Kir2.1-derived tryptic peptides (Figure 7). The SIM analysis detected both unmodified peptides containing the Cys54 or Cys76 residues but only detected the ion at *m/z* 779.8 Da, corresponding to the nitrosylated Cys76 peptide (Figure 7B), as revealed by comprehensive analysis of fragmentation spectra (Figure 7C). No nitrosylated Cys54 peptide was found in the expected retention time (Figure 7B, arrow). These results suggest that the primary sequence surrounding Cys76 promotes its selective S-nitrosylation.

S-Nitrosylation of Kir2.1 in Response to Changes in Myocardial NO Concentrations

To test the effects of changes in myocardial NO concentrations on the *S*-nitrosylation level of Kir2.1 channels we followed 2 experimental strategies. First, we tested the effects of the increase of the NO concentration in mouse ventricular samples. Putative Kir2.1 *S*-nitrosylated protein was labeled with biotin and detected with streptavidin-peroxidase following the biotin-switch assay.[8,9] Representative Western blot demonstrated that in mouse ventricle treatment with 200 μmol/L SNAP increased the *S*-nitrosylation of several proteins including Kir2.1, which was identified by a parallel Western blot with Kir2.1 antibodies (Online Figure III).

Secondly, we tested the effects of a decrease in the myocardial NO concentration. Oxidative stress in the setting of chronic atrial fibrillation (cAF) markedly reduces atrial NO concentrations.[14] Preliminary analysis of the *S*-nitrosylation level of Kir2.1 was done by developing a biotin-switch assay in right atrial appendages obtained from patients in SR and cAF. Figure 8A and 8B suggests that *S*-nitrosylated Kir2.1 proteins were less abundant in samples from cAF patients even when Kir2.1 proteins are expected to be more abundant in those samples.[15]

Discussion

In the present report, we demonstrate that NO, at physiological concentrations, increases $I_{Kir2.1}$ by augmenting the open probability of the channel as a result of the *S*-nitrosylation of Cys76. The findings provide a deeper insight into the modulation of cardiac I_{K1} and describe, for the first time, an important mechanism by which NO participates in the regulation of cardiac RMP and in shaping APs.

NO Increases $I_{Kir2.1}$

Two NO donors (SNAP and DEANO) and an NO-saturated solution induced a concentration-dependent increase of both inward and outward $I_{Kir2.1}$. The fact that the effects were quantitatively and qualitatively similar when using the NO solution and the donors strongly suggests that the increase of $I_{Kir2.1}$ is exclusively mediated by NO and does not involve other NO-independent mechanisms.

It is well established that Kir2.1 channel conductance and inward rectification are strongly dependent on the $[K^+]_o$.[1,2] Indeed, inward rectifier channel blockade induced by Mg^{2+} or polyamines is modulated by changes in the $[K^+]_o$.[1,2] Our experiments demonstrated that NO-induced increase was apparent at low and high $[K^+]_o$, suggesting that the mechanism responsible for the effect does not interfere with the binding site of K^+ to the channel.[1] Moreover, we also showed that NO did not modify the E_K, indicating that it did not change the K^+ selectivity of the channel.

Single-channel experiments demonstrated that NO did not modify the unitary current amplitude, but increased the P_o as a consequence of a ≈3-fold increase of the f_o in spite of a significant reduction in the τ_o. These results clearly pointed to an effect of NO on the channel gating rather than an increase of the number of functional channels and suggest that NO facilitates the close-to-open transition and accelerates the channel closing kinetics.

Posttranslational Modifications Responsible for the NO-Induced Increase

Our results demonstrated that the effects of NO on $I_{Kir2.1}$ and I_{K1} are mediated by a posttranslational modification that depends on the redox state of the cell, because they were abolished by the reducing agent DTT. Among these modifications, *S*-nitrosylation of Cys residues is considered the most

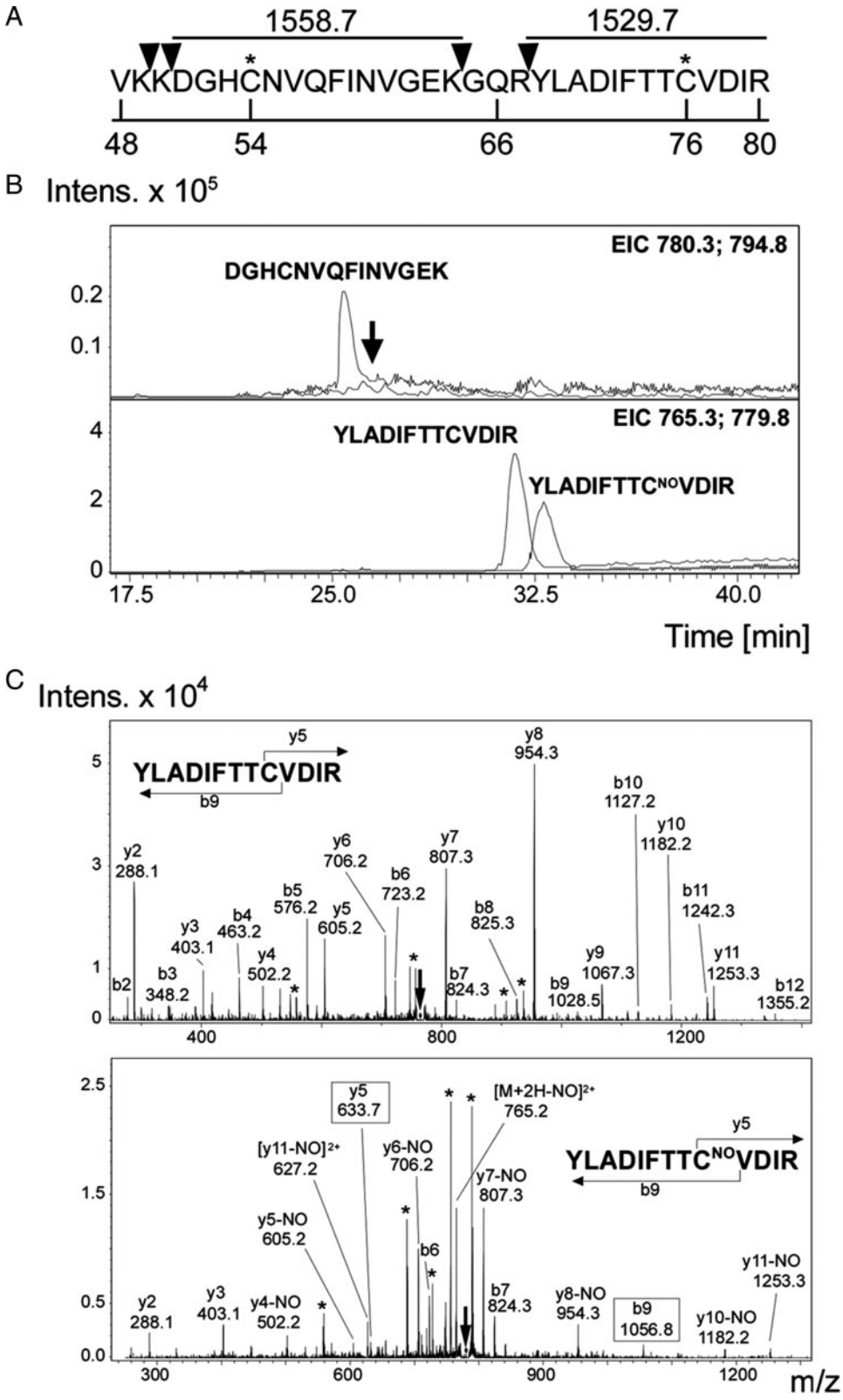

Figure 7. Characterization of the nitrosylation site in Kir2.1 peptide by LC-MS. A, Sequence of peptide Kir2.1Cyt (residues 48 to 80 from cytoplasmic tail) showing the potential trypsin cleavage sites (triangles) and the monoisotopic masses of the longer Kir2.1Cyt-derived tryptic peptides. B, SIM chromatograms for doubly charged Kir2.1-derived tryptic peptides masses at *m/z* 780.3 and 794.8 Da (unmodified and nitrosylated Cys54) (top) and at *m/z* 765.3 and 779.8 Da (unmodified and nitrosylated Cys76) (bottom). Black arrow indicates the expected retention time for nondetected Cys54 nitrosylated peptide. C, Fragmentation spectra from Cys76-unmodified (top) and Cys76-nitrosylated (bottom) Kir2.1 tryptic peptide. Diagram shows fragment ions corresponding to main fragmentation series (b-amino and y-carboxy). * indicates water loss; 2+, doubly charged fragments. Parental ion from each peptide is marked with an arrow. Numbered boxes indicate nitrosylation as revealed by both b and y series.

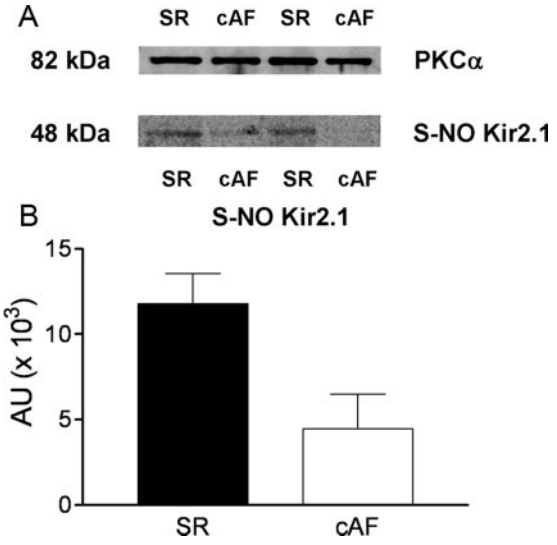

Figure 8. *S*-Nitrosylation of myocardial Kir2.1. A, Representative Western blots showing *S*-nitrosylated Kir2.1 in right atrial appendage obtained from patients in SR or cAF. Protein kinase Cα (PKCα) (top) was used as a loading control. B, Densitometric analysis of the Western blots. Results are presented as the mean±SEM of 2 patients in each group.

important because of its high reactivity, occurrence at physiological conditions, and influence on many protein functions.[11] Our site-directed mutagenesis analysis demonstrated that NO increase of $I_{Kir2.1}$ was mediated by its specific and selective interaction with Cys76. Selective *S*-nitrosylation of one of many available Cys residues in a protein can be achieved through many mechanisms, including the existence of a favorable chemical context for reaction with NO.[11] This mechanism would involve the existence of an acid–base flanking consensus motif and electrostatic interactions with appropriately oriented aromatic amino acid side chains. This chemical context can be provided by adjacent residues in the primary sequence or just in the proximity in the 3D structure.[11] In this regard, in the primary sequence Cys76 is surrounded by 2 Asp (71 and 78) and 1 Arg (80), and it is preceded by an aromatic amino acid (Phe73) that could act as catalysts for *S*-nitrosylation. Furthermore, a Kir2.1 homology model based on the crystal structure of KirBac1.1[16] shows that in the 3D structure the thiol group of Cys76 is surrounded at less than 6 Å by the carboxyl groups of those Asp. SIM analysis of the Kir2.1Cyt peptide demonstrated the selective *S*-nitrosylation of Cys76, and not of Cys54, suggesting that acid–base interactions with neighboring group in the primary sequence and the close presence of the aromatic moiety determine the selective *S*-nitrosylation of Cys76. It is interesting to note that Cys76 belongs to a common highly conserved motif (74-TTxxDxxWR-83) located in the N terminus in close proximity to the first transmembrane segment in the Kir superfamily.[12] Some residues of this mildly hydrophobic area (Q region) are located within an amphipathic α-helical domain termed "slide helix" that runs parallel to the inner leaflet of the plasma membrane.[17] The slide helix is organized so that hydrophilic and hydrophobic residues are located in opposites sides with Cys76 centered on the hydrophobic face.[12] It must be considered that local hydrophobicity might also promote specific *S*-nitrosylation of Cys that belong to protein domains that reside in a juxtamembrane zone.[11] Therefore, the hydrophobic environment in which Cys76 is involved could also contribute to its specific *S*-nitrosylation.

The slide helix has been proposed to be essential for proper channel gating.[16] In fact, several mutations causing Andersen–Tawil syndrome affect residues located in this region.[17] Furthermore, Cys76 has already been reported to be involved in the gating and conduction properties of Kir2.1 channels. Indeed, its mutation to charged/polar amino acids abolishes channel activity because of the destabilization of the open state.[12]

The NO effects were only apparent in Kir2.1 channels in which the 4 subunits contain the Cys76 and not in WT+C76L channels. This is consistent with the observation that the 4 subunits in the Kir channels function in a highly cooperative way.[18] Moreover, Cys76 is highly conserved in the Kir2 family, also being present in Kir2.2 (Cys75) and Kir2.3 (Cys50) channels. In fact, both $I_{Kir2.2}$ and $I_{Kir2.3}$ were also increased by SNAP in a similar extent than $I_{Kir2.1}$ (Online Figures IV and V). This could explain why the NO-induced increase was also observed in the human atrial I_{K1}, where the relative contribution of Kir2.2 and Kir2.3 seems to be even greater than that of Kir2.1.[4]

Potential Physiological Significance

The results obtained in human atrial myocytes strongly suggest that the current increased by NO is I_{K1}. However, the SNAP-increased Ba^{2+}-sensitive current seemed to display less inward rectification than I_{K1}, which could suggest the involvement of other inward rectifying currents. Under our experimental conditions (in the presence of glibenclamide and atropine), activation of I_{KATP} and I_{KACh} is very unlikely; however, we cannot rule out that NO increases other currents, particularly the constitutively active I_{KACh}, which is not inhibited by atropine.

Physiological myocardial NO levels display rapid fluctuations within the cardiac cycle, ranging from 0.26 μmol/L during the systole to 0.93 μmol/L during the diastole.[19] The NO concentrations used in this study (≈0.2 μmol/L) are in the lower range of cardiac NO concentrations, indicating that Kir2.1 channels exhibit a high affinity for NO. Many cardiovascular diseases are accompanied by significant changes in the myocardial NO production and/or bioavailability.[7] For instance, a decrease in cAF[14] and an increase during early ischemia and early reperfusion have been described.[7] Our data suggest that in those diseases in which the NO concentration decreases, Kir2.1 channels would be less *S*-nitrosylated, an effect that, in turn, would decrease the I_{K1}. The contrary would be expected in those cardiovascular diseases in which myocardial NO markedly increases. Preliminary support to this hypothesis was obtained from the biotin-switch assay performed in a reduced number of samples of right atrial appendages obtained from SR and cAF patients. Further confirmation of these results would imply that the decrease in atrial NO concentrations will decrease the I_{K1}. However, it has been demonstrated that cAF increases the Kir2.1 expression level and the I_{K1} density.[15] Thus, it

seems that in cAF the regulation of the expression level of Kir2.1 proteins and their posttranslational modification by *S*-nitrosylation operate in opposite directions. The putative role of the decrease in atrial NO concentrations in promoting or preventing the arrhythmia merits further detailed analysis.

I_{K1} plays a key role in cardiac electrophysiology by stabilizing the RMP and shaping the initial and the final phase of the atrial and ventricular AP.[1] Therefore, modulation of I_{K1} would have profound effects on cardiac excitability and arrhythmogenesis.[2] Conduction of the cardiac impulses depends on active and passive membrane properties. The slight hyperpolarization of the RMP produced by NO would influence both membrane properties because it would simultaneously increase the voltage-dependent Na^+ channel availability, decrease the resting membrane resistance, and impair the approach toward threshold potentials. The first effect would tend to increase, the other 2 to reduce cardiac excitability and conduction velocity. Furthermore, the strong outward component of the I_{K1} during repolarization rapidly restores the membrane potential to resting values. The increase of the I_{K1} outward component is probably responsible for the marked shortening of the final phase of AP repolarization produced by NO in mouse[8] and human atria. This shortening would critically influence the refractory period. Moreover, the importance of I_{K1} in the establishment of a fast and stable reentry of a rotor has been demonstrated.[6] The prediction is that I_{K1} helps to abbreviate the APD near the center of rotation (core); in addition, I_{K1} is also essential in maintaining the stability of these rotors.[2,6]

Therefore, it can be concluded that the I_{K1} increase produced by the specific *S*-nitrosylation of Cys76 of Kir2.1 channels represents an important mechanism by which NO participates in the control of cardiac excitability under physiological conditions. Furthermore, this redox-related modulation is attributable to an increase in the opening frequency of Kir2.1 channels that exhibit an unexpected high affinity for this gaseous mediator.

Acknowledgments

We thank Dr Antonio Rodríguez Artalejo for his helpful suggestions.

Sources of Funding

Supported by Ministerio de Educación y Ciencia (SAF2005-04609, SAF2008-04903); Ministerio de Sanidad y Consumo; Instituto de Salud Carlos III (Red HERACLES RD06/0009 and PI080665); Fundación LILLY; and Centro Nacional de Investigaciones Cardiovasculares (CNIC-13). R.G. is a fellow of Comunidad Autónoma de Madrid.

Disclosures

None.

References

1. Lopatin AN, Nichols CG. Inward rectifiers in the heart: an update on I_{K1}. *J Mol Cell Cardiol*. 2001;33:625–638.
2. Dhamoon AS, Jalife J. The inward rectifier current I_{K1} controls cardiac excitability and is involved in arrhythmogenesis. *Heart Rhythm*. 2005;2:316–324.
3. Wang Z, Yue L, White M, Pelletier G, Nattel S. Differential distribution of inward rectifier potassium channel transcripts in human atrium versus ventricle. *Circulation*. 1998;98:2422–2428.
4. Gaborit N, Le Bouter S, Szuts V, Varro A, Escande D, Nattel S, Demolombe S. Regional and tissue specific transcript signatures of ion channel genes in the non-diseased human heart. *J Physiol*. 2007;582:675–693.
5. Morita H, Wu J, Zipes DP. The QT syndromes: long and short. *Lancet*. 2008;372:750–763.
6. Noujaim SF, Pandit SV, Berenfeld O, Vikstrom K, Cerrone M, Mironov S, Zugermayr M, Lopatin AN, Jalife J. Up-regulation of the inward rectifier K^+ current (I_{K1}) in the mouse heart accelerates and stabilizes rotors. *J Physiol*. 2007;578:315–326.
7. Schulz R, Rassaf T, Massion PB, Kelm M, Balligand JL. Recent advances in the understanding of the role of nitric oxide in cardiovascular homeostasis. *Pharmacol Ther*. 2005;108:225–256.
8. Gómez R, Núñez L, Vaquero M, Amorós I, Barana A, de Prada T, Macaya C, Maroto L, Rodríguez E, Caballero R, López-Farré A, Tamargo J, Delpón E. Nitric oxide inhibits Kv4.3 and human cardiac transient outward potassium current I_{to1}. *Cardiovasc Res*. 2008;80:375–384.
9. Núñez L, Vaquero M, Gómez R, Caballero R, Mateos-Cáceres P, Macaya C, Iriepa I, Gálvez E, López-Farré A, Tamargo J, Delpón E. Nitric oxide blocks hKv1.5 channels by S-nitrosylation and by a cyclic GMP-dependent mechanism. *Cardiovasc Res*. 2006;72:80–89.
10. Piao L, Li J, McLerie M, Lopatin AN. Cardiac I_{K1} underlies early action potential shortening during hypoxia in the mouse heart. *J Mol Cell Cardiol*. 2007;43:27–38.
11. Hess DT, Matsumoto A, Kim SO, Marshall HE, Stamler JS. Protein S-nitrosylation: purview and parameters. *Nat Rev Mol Cell Biol*. 2005;6:150–166.
12. Garneau L, Klein H, Parent L, Sauvé R. Contribution of cytosolic cysteine residues to the gating properties of the Kir2.1 inward rectifier. *Biophys J*. 2003;84:3717–3729.
13. Lu T, Nguyen B, Zhang X, Yang J. Architecture of a K^+ channel inner pore revealed by stoichiometric covalent modification. *Neuron*. 1999;22:571–580.
14. Kim YM, Guzik TJ, Zhang YH, Zhang MH, Kattach H, Ratnatunga C, Pillai R, Channon KM, Casadei B. A myocardial Nox2 containing NAD(P)H oxidase contributes to oxidative stress in human atrial fibrillation. *Circ Res*. 2005;97:629–636.
15. Dobrev D, Graf E, Wettwer E, Himmel HM, Hála O, Doerfel C, Christ T, Schüler S, Ravens U. Molecular basis of downregulation of G-protein-coupled inward rectifying K^+ current $I_{K,ACh}$ in chronic human atrial fibrillation: decrease in GIRK4 mRNA correlates with reduced $I_{K,ACh}$ and muscarinic receptor-mediated shortening of action potentials. *Circulation*. 2001;104:2551–2557.
16. Kuo A, Gulbis JM, Antcliff JF, Rahman T, Lowe ED, Zimmer J, Cuthbertson J, Ashcroft FM, Ezaki T, Doyle DA. Crystal structure of the potassium channel KirBac1.1 in the closed state. *Science*. 2003;300:1922–1926.
17. Decher N, Renigunta V, Zuzarte M, Soom M, Heinemann SH, Timothy KW, Keating MT, Daut J, Sanguinetti MC, Splawski I. Impaired interaction between the slide helix and the C-terminus of Kir2.1: a novel mechanism of Andersen syndrome. *Cardiovasc Res*. 2007;75:748–757.
18. Nekouzadeh A, Silva JR, Rudy Y. Modeling subunit cooperativity in opening of tetrameric ion channels. *Biophys J*. 2008;95:3510–3520.
19. Malinski T. Understanding nitric oxide physiology in the heart: a nanomedical approach. *Am J Cardiol*. 2005;96:13i–24i.

Circulation Research
JOURNAL OF THE AMERICAN HEART ASSOCIATION

Nitric Oxide Increases Cardiac I_{K1} by Nitrosylation of Cysteine 76 of Kir2.1 Channels

Ricardo Gómez, Ricardo Caballero, Adriana Barana, Irene Amorós, Enrique Calvo, Juan Antonio López, Helene Klein, Miguel Vaquero, Lourdes Osuna, Felipe Atienza, Jesús Almendral, Ángel Pinto, Juan Tamargo and Eva Delpón

Circ Res. 2009;105:383-392; originally published online July 16, 2009;
doi: 10.1161/CIRCRESAHA.109.197558
Circulation Research is published by the American Heart Association, 7272 Greenville Avenue, Dallas, TX 75231

Print ISSN: 0009-7330. Online ISSN: 1524-4571

Online Data Supplement

Expanded Material and Methods

Human atrial myocyte isolation

The study was approved by the Investigation Committee of the Hospital Universitario Gregorio Marañón (CNIC-13) and conforms with the principles outlined in the Declaration of Helsinki. Each patient gave written informed consent. Data regarding age, sex, type of surgery, and pharmacological treatment of the patients are included in the online Table I.

Human right atrial specimens were obtained from patients (n=11) undergoing cardiac surgery. Atrial myocytes were enzimatically isolated following previously described methods.[1,2] In brief, samples were immediately placed into chilled Ca^{2+}-free Tyrode's solution containing (mmol/L): NaCl 100, KCl 10, KH_2PO_4 1.2, $MgSO_4$ 5, taurine 50, MOPS 5, and glucose 20 (pH 7.0 with NaOH) and supplemented with 2,3-butanedione monoxime (BDM, 30 mmol/L), chopped into small pieces (≈1 mm^3), and washed 3 times for 3 minutes with Ca^{2+}-free Tyrode's solution. Tissue pieces were then changed to Ca^{2+}-free solution containing 254 U/mL collagenase type I (Worthington, USA) and 0.5 mg/mL protease type XXIV (Sigma Chemical Co, United Kingdom) and gently stirred for 15 minutes. Afterwards, the Ca^{2+} concentration was raised to 0.2 mmol/L, and the tissue was stirred for 30 minutes more. Stirring was continued with Tyrode's solution (0.2 mmol/L Ca^{2+}) containing only collagenase until rod-shaped striated myocytes were seen (≈35 minutes). During all these steps, the solutions were continuously oxygenated with 100% O_2 at 37°C. Myocytes were kept until use in a storage solution containing (mmol/L): KCl 20, KH_2PO_4 10, glucose 10, K-glutamate 70,

β-hidroxybutyrate 10, taurine 10, EGTA 10, and albumin 1 (pH 7.4 with KOH). Myocytes were used for electrophysiological recordings within 8 h.

Kir2.1 constructs and cell transfection

Human Kir2.1 wild type (WT), a mouse Kir2.1 channel in which six Cys (C54V, C76V, C89I, C101L, C149F, and C169V) were mutated simultaneously (IRK1J), human Kir2.2, Kir2.3, and C169A cDNA were kindly provided by Dr. J. Jalife (Michigan University, USA), Dr. J. Yang (Columbia University, USA), and Dr. J. Sánchez-Chapula (Colima University, México), respectively, and were subcloned into pcDNA3.1 plasmid (Invitrogen, USA). C54S, C76L, C76V, C89G, C101S, and C149S Kir2.1 mutations were introduced using the QuikChange Site-Directed Mutagenesis kit (Stratagene, USA) and subcloned into pMT21 plasmid.[3]

CHO cells were cultured and transfected as previously described.[2,4-7] Cells were grown in Ham-F12 medium supplemented with 10% fetal bovine serum, 100 U/ml penicillin, and 100 μg/ml streptomycin. The cultures were passaged every 4–5 days using a brief trypsin treatment. CHO cells were transiently transfected with the cDNA encoding Kir2.1, Kir2.2, and Kir2.3 channels (1.6 μg) together with the cDNA encoding the CD8 antigen (0.5 μg) by using FUGENE6 (Roche Diagnostics, Switzerland) following manufacturer instructions. For culture and transfections, 50 mm culture dishes were used. After 48 h, cells were incubated with polystyrene microbeads precoated with anti-CD8 antibody (Dynabeads M450; Dynal, Norway). Most of the cells that were beaded also had channel expression. The cells were removed from the dish with a cell scraper and the cell suspension was stored at room temperature and used within 12 h for electrophysiological experiments.

Recording techniques

Macroscopic current recordings

A small aliquot of cell suspension was placed in a 0.5 ml chamber mounted on the stage of an inverted microscope (Nikon TMS, Nikon Co., Japan). After settling to the bottom of the chamber, cells were perfused at 1 $ml \cdot min^{-1}$ with external solution (see composition below).

Macroscopic currents were recorded at room temperature (21-23ºC) using the whole-cell patch-clamp technique using an Axopatch-200B patch clamp amplifier (Molecular Devices, Foster City, CA, USA).[2,4-8] Recording pipettes were pulled from 1.0 mm o.d. borosilicate capillary tubes (GD1, Narishige Co., Ltd, Japan) using a programmable patch micropipette puller (Model P-2000 Brown-Flaming, Sutter Instruments Co., USA) and were heat-polished with a microforge (Model MF-83, Narishige). Micropipette resistance was <3.5 MΩ when filled with the internal solution and immersed in the external solution. The capacitive transients elicited by symmetrical 10 mV steps from 0 mV were recorded at 50 kHz (filtered at 10 kHz) for subsequent calculation of capacitative surface area, access resistance and input impedance. In all the experiments, series resistance was compensated manually by using the series resistance compensation unit of the Axopatch amplifier, and ≥80% compensation was achieved. In CHO cells, uncompensated access resistance and cell capacitance were 1.5±0.2 MΩ, and 14.9±0.6 pF, respectively (n=39), whereas mean maximum Kir2.1, Kir2.2, and Kir2.3 current ($I_{Kir2.1}$, $I_{Kir2.2}$, and $I_{Kir2.3}$) amplitudes at -120 mV were 2.8±0.2 (n=31), 1.5±0.1 (n=4), and 0.2±0.03 nA (n=4), respectively. In human atrial myocytes mean maximum I_{K1} amplitude at -100 mV, uncompensated access resistance, and capacitance averaged -448±65 pA, 3.2±0.5 MΩ, and 81.6±13.7 pF (n=24), respectively. Thus, under our experimental conditions no significant voltage errors (<5 mV) due to series resistance

were expected with the micropipettes used. The current recordings were sampled at 4 kHz, filtered at half the sampling frequency and stored on the hard disk of a computer for subsequent analysis.

To record human atrial I_{K1}, the external solution contained (mmol/L): NaCl 120, KCl 20, $CaCl_2$ 1, $MgCl_2$ 1, HEPES 10, 4-aminopyridine 1, $CoCl_2$ 2, glucose 10, and atropine (1 μmol/L) (pH 7.4 with NaOH).[1] In some experiments, the effects of SNAP on the Ba^{2+}-sensitive current were studied. In these experiments, human atrial myocytes were first perfused with control external solution followed by external solution containing 200 μmol/L (±)-*S*-nitroso-*N*-acetylpenicillamine (SNAP, Calbiochem, USA) and finally with external solution containing SNAP and $BaCl_2$ (100 μmol/L). All these solutions were supplemented with atropine and glibenclamide (10 μmol/L). Ba^{2+}-sensitive currents were obtained by digital subtraction of current traces. Recording pipettes were filled with an internal solution containing (mmol/L): K-aspartate 80, KCl 42, KH_2PO_4 10, MgATP 5, phosphocreatine 3, HEPES 5, and EGTA 5 (pH 7.2 with KOH). To record human atrial Na^+/Ca^{2+} exchange current (I_{NCX}), the external solution contained (mmol/L): NaCl 140, CsCl 4, $CaCl_2$ 2.5, $MgCl_2$ 1.2, HEPES 5, glucose 10, glibenclamide (10 μmol/L) and atropine (1 μmol/L) (pH 7.4 with NaOH). Solution was supplemented with 1 μmol/L nifedipine and 10 μmol/L ouabain to inhibit the Ca^{2+} current and the Na^+/K^+ ATPase, respectively. After obtaining control recordings (total current), external solution was changed to a solution containing 5 mmol/L Ni^{2+}/0 Ca^{2+}. I_{NCX} was measured as the Ni^{2+}-sensitive current and was obtained by digital subtraction of Ni^{2+}-insensitive current from total currents. The intracellular solution to record I_{NCX} contained (mmol/L): CsCl 110, NaCl 20, HEPES 10, $MgCl_2$ 0.4, glucose 5, tetraethylammonium chloride 20, EGTA 5, MgATP 4, $CaCl_2$ 1 (pH 7.2 with CsOH).[9] To record $I_{Kir2.1}$, $I_{Kir2.2}$, and $I_{Kir2.3}$, CHO cells were perfused with an external solution

containing (mmol/L): NaCl 136, KCl 4, $CaCl_2$ 1.8, $MgCl_2$ 1, HEPES 10, and glucose 10 (pH 7.4 with NaOH). To obtain 1 and 10 mmol/L extracellular K^+ concentration ($[K^+]_o$) solutions, equimolar substitution between KCl and NaCl was used. The internal solution used for whole-cell current recordings in CHO cells was the same as described for recording human atrial I_{K1} (see above).

Single-channel recordings

Single-channel currents were recorded at room temperature using the cell-attached patch-clamp configuration (Axopatch-200B patch clamp amplifier).[10] Cells were suspended in bath solution (in mmol/L: KCl 140, $CaCl_2$ 1.8, $MgCl_2$ 1, HEPES 10, and glucose 10, pH 7.4 with KOH). Patch pipettes were pulled from 1.5 mm o.d. borosilicate capillary tubes (Harvard Apparatus Ltd, USA), coated at the tip with Sylgard (Dow Corning, USA), and fire-polished with a microforge. When filled with pipette solution (in mmol/L: KCl 140, $CaCl_2$ 1, and HEPES 10; pH 7.4 with KOH), tip resistances were between 5 and 10 MΩ. Patches with more than one channel were discarded.

Action potentials

Action potentials were recorded from isolated human atrial myocytes in current clamp configuration using an Axopatch 200B patch clamp amplifier.[1] Myocytes were perfused with an external solution containing (mmol/L): NaCl 150, KCl 5.4, MgCl 2, $CaCl_2$ 2, glucose 10, and HEPES 10, atropine (1 μmol/L), and glibenclamide (10 μmol/L) (pH 7.4 with NaOH). Recording pipettes were pulled from 1.0 mm o.d. borosilicate capillary tubes and filled with internal solution containing (mmol/L): K-aspartate 100, NaCl 8, KCl 40, Mg-ATP 5, EGTA 5, CaCl2 2, GTP 0.1, and HEPES 10

(pH 7.4 with KOH). Tip resistance was >7 MΩ to ensure high quality gigaseals and minimal depolarization of membrane potential.

Pulse protocols and analysis

The protocol to record human atrial I_{K1} consisted of 50-ms steps from a holding potential of -80 mV to -100 mV followed by depolarizing ramps to -10 mV (800 ms).[1] For macroscopic $I_{Kir2.1}$ recorded in the presence of 4 and 10 mmol/L $[K^+]_o$, the protocol to obtain current-voltage (I-V) curves consisted of 250 ms-pulses in 10 mV increments from a holding potential of –60 mV to potentials between −120 and +20 mV. At 1 mmol/L $[K^+]_o$, $I_{Kir2.1}$ was recorded by applying 250 ms-pulses from –60 mV to potentials ranging –150 and –10 mV. The protocol to obtain $I_{Kir2.2}$ and $I_{Kir2.3}$ I-V curves consisted of 250 ms-pulses in 10 mV increments from –60 mV to potentials between −120 and +20 mV.

The current amplitude was measured at the end of the pulse. All the I-V curves were corrected according to the calculated liquid junction potentials (LJP): 13.5, 13.2, 12.5, 12.1 mV at 1, 4, 10, and 20 mmol/L $[K^+]_o$, respectively.[11]

To obtain the EC_{50} (concentration that produces the half maximum response) and the Hill coefficient (n_H) the increase produced by SNAP at various concentrations [*D*] was fitted to the equation: $f = E_{min} + (E_{max}-E_{min})/\{1+(EC_{50}/[D])^{n_H}\}$.

The protocol to record I_{NCX} consisted of 300 ms-pulses from -40 mV to potentials ranging -80 and +80 mV. I_{NCX} was calculated as the difference between the current measured in the presence of extracellular Ca^{2+} and that measured in the presence of 5 mmol/L Ni^{2+}/0 Ca^{2+}.[9] I-V curves of I_{NCX} were corrected according to a LJP of 15.7 mV.

Single-channel currents were recorded by applying 1 s pulses to -80 mV (from a holding potential of 0 mV),[10] amplified, digitized at 10 kHz, and stored on the hard disk

of a computer for subsequent analysis. The recordings were filtered at 1 kHz. Data were analyzed using pCLAMP software. Open probability (P_o) was calculated in each experiment by dividing the time that the channel remains in the open state by the total recording time. The opening frequency (f_o) was calculated for each experiment as the inverse of the closed time between events. Amplitude of unitary currents in control conditions and in the presence of 200 μmol/L SNAP were calculated for each experiment from a Gaussian distribution fit to amplitude histograms that were constructed by plotting amplitude data as a function of the number of events per bin (bin width= 0.05 pA). Open and closed-time constants (τ_o and τ_c) were calculated for each experiment from the Gaussian fit to dwell-time histograms that were constructed by plotting dwell-time data as a function of the number of events per bin (10 bins per decade).

Action potentials were elicited by depolarizing current pulses of 2 ms in duration at 1.5 times the current threshold.

Biotin-switch-assay in human right atrial appendage samples

Detection of S-nitrosylated Kir2.1 proteins was performed using the biotin-switch-assay followed by Western blot as described.[2,8] Right atrial appendage samples were obtained from sinus rhythm (n=2) and chronic atrial fibrillation (n=2) patients (online Table I) undergoing cardiac surgery. After excision, atrial appendages were washed in PBS, immediately snap-frozen in liquid nitrogen and stored at −85ºC.

Atrial tissue was homogenized in a non-denaturing solution (in mmol/L: Tris-HCl 50, NaCl 300, EDTA 5, neocuproine 0.1, and 1% Triton X-100, plus 14.6 μL/mL pepstatin and 25 μL/mL leupeptin) using, in the following order: (1) a loose-fitting Dounce homogenizer (10 strokes); (2) an UltraTurrax T-25 tissue grinder (3x10 s bursts); and

(3) a Branson 250 sonicator (3x20 s bursts). Nuclei and cell debris were removed by centrifugation at 5000 *g* for 10 min at 4ºC.

The total protein amount of the extracts was calculated with the bicinchonic acid method (BCA, Pierce, USA) and each extract was then adjusted to 0.5 mg/mL of protein. The extracts were precipitated with 2 volumes of cold acetone (3500 *g*, 10 min, 4ºC) and the pellets were resuspended in non-denaturing solution (80 μL) before incubating with 4 volumes of blocking buffer (in mmol/L: HEPES 225, EDTA 0.9, neocuproine 0.09, methyl-methanethiosulfonate 20, and 2.5% SDS) for 20 min at 50ºC with agitation. After blocking, extracts were precipitated with 10 volumes of cold acetone and resuspended in 0.1 mL of HENS buffer (in mmol/L: HEPES 250, EDTA 1, neocuproine 0.1 and 1% SDS) per mg of protein. Subsequently, extracts were incubated with 1/3 volume of 4 mM N-[6-(biotinamido)hexyl]-3´-(2´-pyridyldithio)propionamide (biotin-HPDP, Pierce) and 1 mmol/L ascorbate for 1 h at room temperature. After another cold acetone precipitation, the pellet was resuspended in 4 μL of HENS buffer.

To detect biotinylated proteins by Western blot, samples were separated on denaturing SDS 10% polyacrylamide gels, transferred to nitrocellulose membranes using a semi-dry transfer system, blocked with nonfat dried milk, and incubated with streptavidin-peroxidase (1:2000; General Electric Healthcare, USA) for 1 h. Since the Cys biotinylation is highly reversible, samples were prepared without reducing agents. To prevent biotin-HPDP non-specific reactions, samples were not boiled before electrophoresis. All the procedures preceding electrophoresis were carried out in darkness. Equal loading of the blots was confirmed by a parallel Western blot performed with protein kinase C-α antibody (1:500; Santa Cruz Biotechnology, USA) since the expression of protein kinase C is not modified in chronic atrial fibrillation.[12]

Biotin-switch-assay in mouse ventricle

Ventricular tissue was homogenized as described above for human atrial samples. The total protein amount of the extracts was also calculated with the BCA method and each extract was then adjusted to 0.5 mg/mL of protein. Afterwards, extracts were incubated with 200 μmol/L SNAP for 15 min in darkness. SNAP was removed by precipitation and centrifugation (3500 g, 10 min) with 2 volumes of cold acetone at 4ºC. The pellets were resuspended in non-denaturing solution (80 μL) to perform the biotin-switch-assay as described above. To detect biotinylated proteins a Western blot was performed as described for human atrial samples. A parallel gel (SDS-PAGE 10%) was developed to determine the expression of Kir2.1 protein. Nitrocellulose membrane was incubated for 1 h with an anti-Kir2.1 antibody (1:800; Santa Cruz Biotechnology) and then for 30 min with a horseradish peroxidase-conjugated secondary antibody (1:5000; Santa Cruz Biotechnology). Protein expression was detected by chemoluminescence (ECL, General Electric Healthcare).

Drugs

The NO donors SNAP and N,N-diethylamine-diazenolate-2-oxide (DEANO, Sigma) were initially dissolved in ethanol and water, respectively, to yield 10 mmol/L stock solutions. Donor solutions and the NO-saturated solution were prepared freshly for each experiment.[2,8] To prepare the NO solution, the external solution was first bubbled with argon (Ar) for 20–30 min in a gas washing bottle obtaining an O_2-free solution and, then, with NO (450 ppm NO/Ar). The pH of the solution was adjusted to 7.4 with NaOH. In a separate group of experiments, the NO concentration in the recording chamber was measured at the same perfusion flow rate using a potentiometric NO sensor coupled to an ISO-NO Mark II Isolated Nitric Oxide Meter (World Precision

Instruments Inc., United Kingdom).[2,8,13] Real-time NO measurements were recorded using data acquisition hardware and data recording software Chart v4.1.2 (Powerlab and AD Instruments, Panlab, Spain). The electrode was calibrated daily according to the manufacturer instructions by the conversion of known concentrations of $NaNO_2$ into NO in the presence of H_2SO_4 and KI. Ditiothreitol, glibenclamide, ouabain, atropine, and nifedipine were purchased from Sigma as a powder and dissolved as appropriate to yield 0.01 M stock solutions. Further dilutions were carried out in external solution to obtain the desired final concentration. Control solutions always contained the same solvent concentrations as the test solution.

Characterization of S-nitrosylation by liquid chromatography coupled online to tandem-mass spectrometry (LC-MS)

A synthetic peptide spanning the sequence 48-VKKDGHCNVQFINVGEKGQRYLADIFTTCVDIR-80 from the cytoplasmic tail of Kir2.1 (Kir2.1Cyt, 20 μg), was dissolved in ammonium bicarbonate (50 mmol/L) and incubated with SNAP (200 μmol/L) for 15 min at room temperature in darkness. Afterwards, the peptide was digested by adding 0.5 μg of modified porcine trypsin (sequencing grade; Promega, USA) at 37°C for 30 min. The resulting tryptic peptides were online injected onto a C-18 reversed-phase nanocolumn (Mediterranean Sea 18; Teknokroma, Spain) and analyzed in a continuous acetonitrile gradient. A flow rate of *ca*. 300 nL/min was used to elute peptides from the reversed-phase nanocolumn to an electrospray ion source, coupled to an ion trap mass spectrometer (Esquire HCT; Bruker Daltonics, Germany) for real-time ionization and fragmentation. Single Ion Monitoring (SIM) experiments were done for the masses corresponding to the unmodified and

nitrosylated-tryptic peptides. A 3 Da window was set for ion isolation, and collision energy of 0.90 V was used for peptide fragmentation.[14]

Statistical methods

Results are expressed as mean±SEM. Paired or unpaired *t* test or one-way ANOVA followed by Newman-Keuls test were used to assess statistical significance where appropriate. A value of $P<0.05$ was considered significant.

Expanded Results

Online Figure I. Effects of SNAP on I_{NCX} recorded in human atrial myocytes.

(A) Representative background current traces recorded by applying 300 ms-pulses from a holding potential of -40 mV to potentials ranging -80 and +80 mV (total current) and I_{NCX} (Ni^{2+}-sensitive current), in the absence and presence of 200 μmol/L SNAP. (B) Mean I-V curves of total background and Ni^{2+}-insensitive currents in the absence and presence of SNAP. (C) Mean I-V curves of Ni^{2+}-sensitive currents (I_{NCX}) in the absence and presence of SNAP. In B and C, the I-V curves have been corrected according to a LJP of 15.7 mV. The NO donor did not modify either the Ni^{2+}-sensitive or the Ni^{2+}-insensitive currents recorded in human atrial myocytes (n=6, P>0.05) indicating that the contribution of I_{NCX} to the NO-induced I_{K1} increase can be ruled out.

Online Figure I

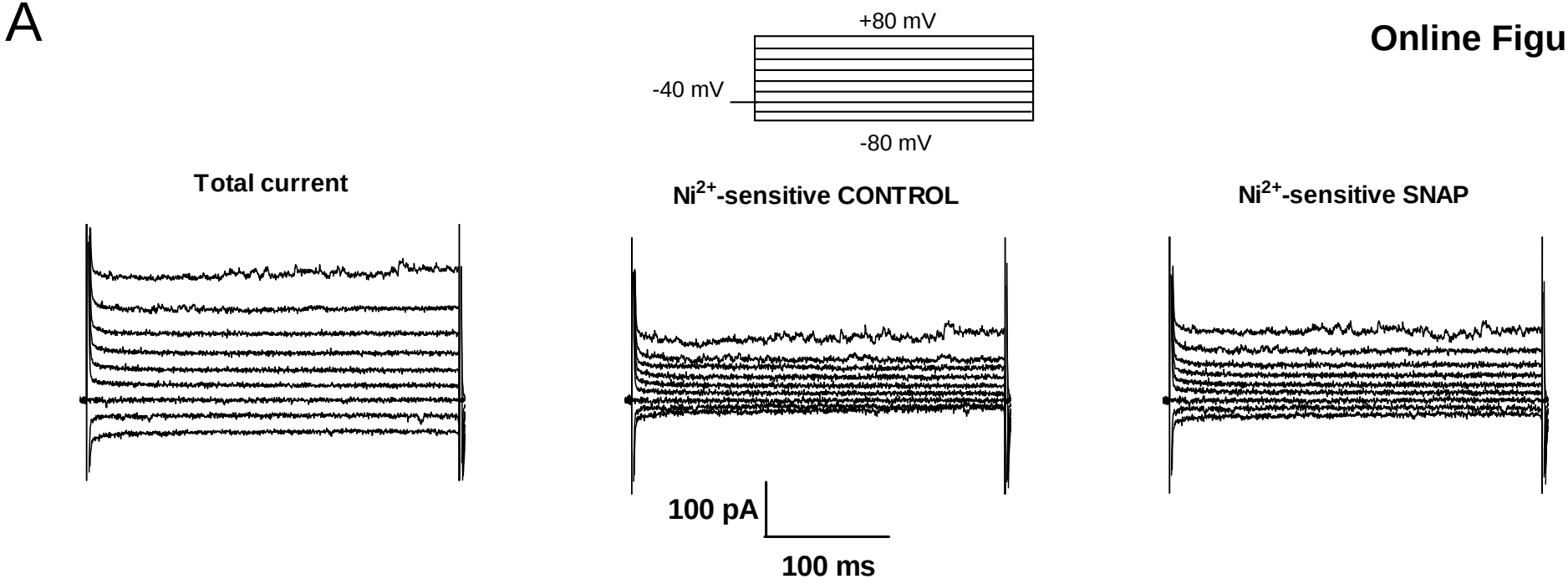

Online Figure II. Effects of SNAP on unitary Kir2.1 currents.

(A) Example of amplitude histograms at -80 mV obtained in one CHO cell expressing Kir2.1 channels under control conditions and in the presence of 200 μmol/L SNAP constructed by plotting amplitude data as a function of the number of events per bin (bin width= 0.05 pA). The fit to a Gaussian distribution yielded discrete peaks at 0.01 pA (closed channels) and -1.60 pA (open channels) in control conditions. In the presence of SNAP, amplitude values were 0.02 and -1.49 pA for closed and open channels, respectively. (B) Amplitude histograms at -80 mV in the absence and presence of SNAP constructed by pooling amplitude data from 6 experiments. As can be observed, SNAP did not modify single channel current amplitude but markedly increased the number of events.

Online Figure II

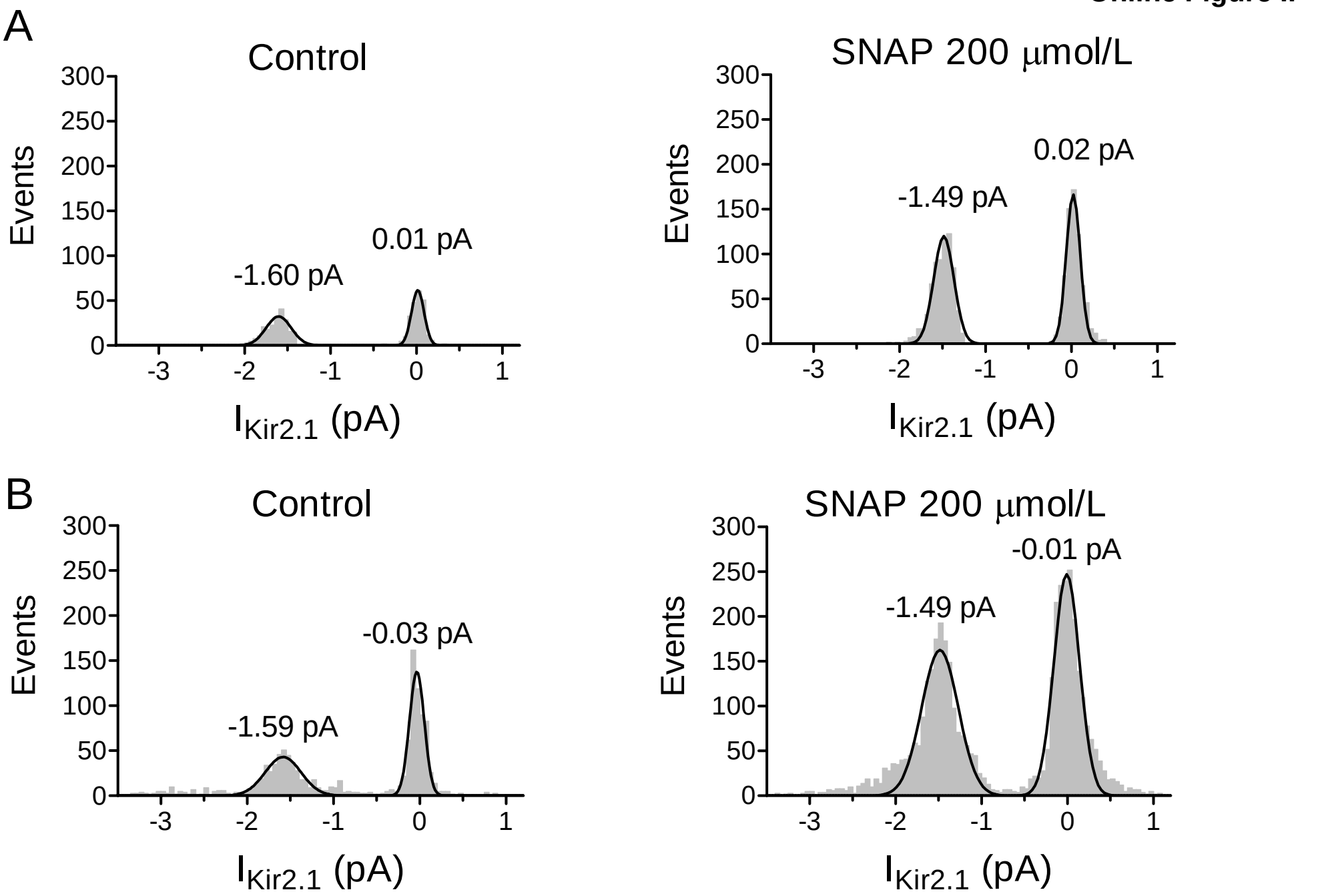

Online Figure III. SNAP produces the S-nitrosylation of Kir2.1 channels in mouse ventricle. (A) Representative Western blots showing S-nitrosylated Kir2.1 (red arrow) in mouse ventricle samples incubated (right lane) or not (left lane) with 200 μmol/L SNAP. (B) Bar graph showing the densitometric scanning of the Western blots. Results are presented as mean±SEM of 4 samples. * $P<0.05$ vs control.

A

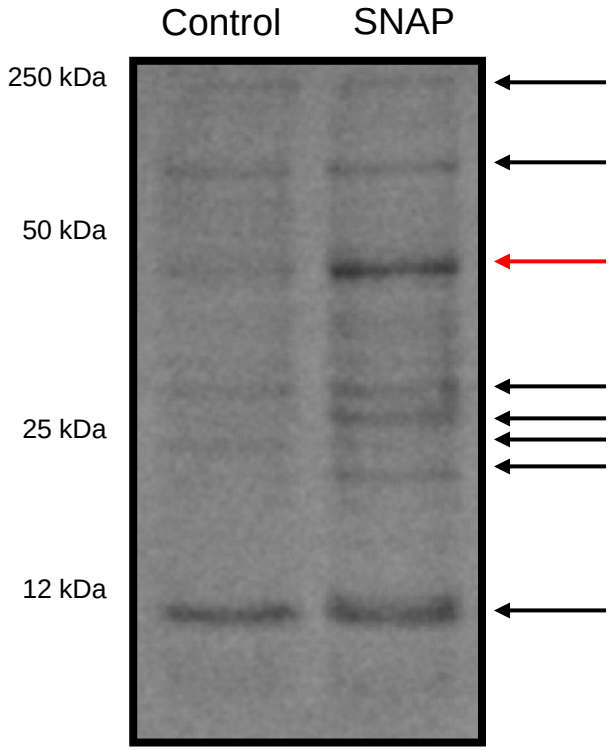

B

Online Figure III

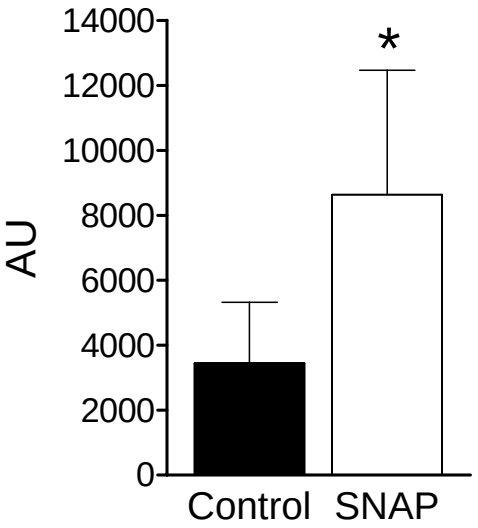

Online Figure IV. Effects of SNAP on Kir2.2 channels.

(A) $I_{Kir2.2}$ traces recorded by applying 250 ms-pulses from a holding potential of -60 mV to potentials ranging -120 and +20 mV in the absence (left) and presence of 200 μmol/L SNAP (right). (B) Mean I-V curves of $I_{Kir2.2}$ in the absence and presence of SNAP. The inset shows data at potentials positive to E_K in an expanded scale. Under control conditions, hyperpolarizing pulses elicited large inward currents, whereas depolarizing pulses elicited small outward currents. SNAP increased $I_{Kir2.2}$ at voltages negative and positive to E_K, reaching a 19.9±3.6% of increase at –120 mV ($P<0.05$, n=4). In the I-V relationship, the voltage is adjusted to the LJP of 13.2 mV.

Online Figure IV

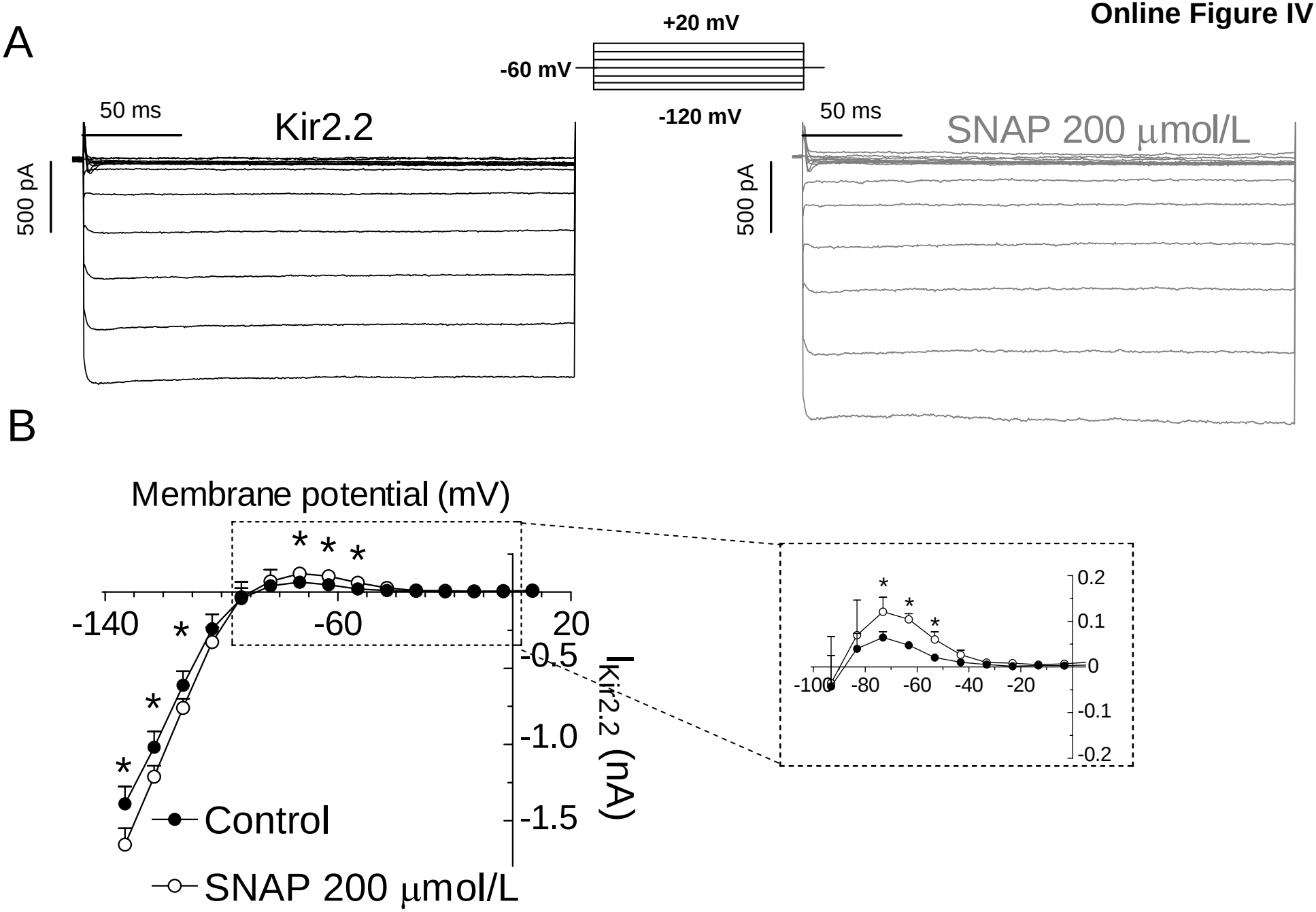

Online Figure V. Effects of SNAP on Kir2.3 channels.

(A) $I_{Kir2.3}$ traces recorded by applying 250 ms-pulses from a holding potential of -60 mV to potentials ranging -120 and +20 mV in the absence (left) and presence of 200 μmol/L SNAP (right). (B) Mean I-V curves of $I_{Kir2.3}$ in the absence and presence of SNAP. The inset shows data at potentials positive to E_K in an expanded scale. In this case, under control conditions, both inward and outward current amplitudes were smaller and inward current kinetics slower than those of $I_{Kir2.1}$ and $I_{Kir2.2}$. SNAP increased $I_{Kir2.3}$ at voltages negative and positive to E_K reaching a 15.7±2.5% of increase at –120 mV ($P<0.05$, n=4). In the I-V relationship, the voltage is adjusted to the LJP of 13.2 mV.

Online Figure V

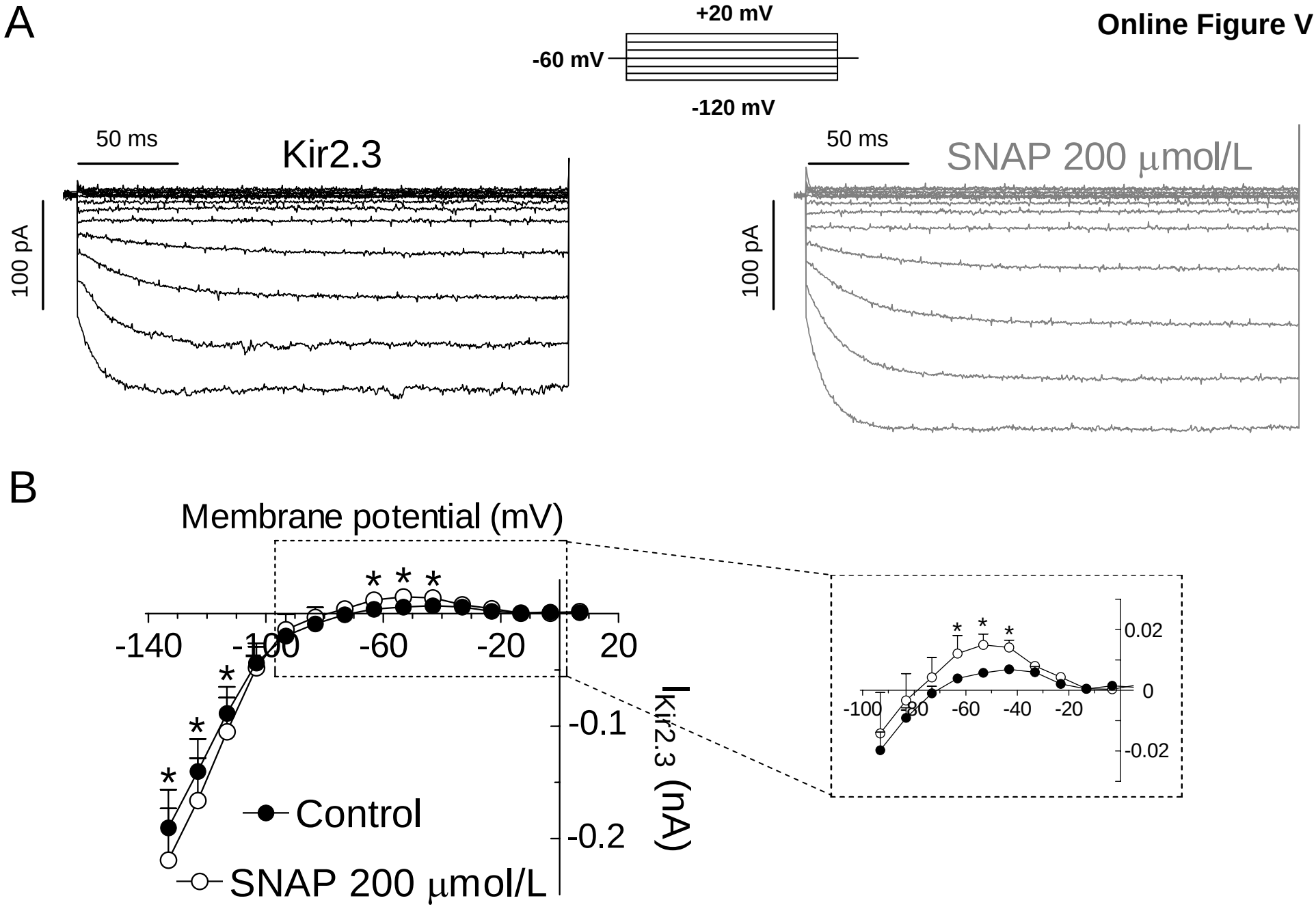

References

1. Dobrev D, Graf E, Wettwer E, Himmel HM, Hála O, Doerfel C, Christ T, Schüler S, Ravens U. Molecular basis of downregulation of G-protein-coupled inward rectifying K^+ current $I_{K,ACh}$ in chronic human atrial fibrillation: decrease in GIRK4 mRNA correlates with reduced $I_{K,ACh}$ and muscarinic receptor-mediated shortening of action potentials. *Circulation*. 2001;104:2551-2557.
2. Gómez R, Núñez L, Vaquero M, Amorós I, Barana A, de Prada T, Macaya C, Maroto L, Rodríguez E, Caballero R, López-Farré A, Tamargo J, Delpón E. Nitric oxide inhibits Kv4.3 and human cardiac transient outward potassium current I_{to1}. *Cardiovasc Res*. 2008;80:375-384.
3. Garneau L, Klein H, Parent L, Sauvé R. Contribution of cytosolic cysteine residues to the gating properties of the Kir2.1 inward rectifier. *Biophys J*. 2003;84:3717-3729.
4. Tutor AS, Delpón E, Caballero R, Gómez R, Núñez L, Vaquero M, Tamargo J, Mayor F Jr, Penela P. Association of 14-3-3 proteins to beta1-adrenergic receptors modulates Kv11.1 K^+ channel activity in recombinant systems. *Mol Biol Cell*. 2006;17:4666-4674.
5. Vaquero M, Caballero R, Gómez R, Núñez L, Tamargo J, Delpón E. Effects of atorvastatin and simvastatin on atrial plateau currents. *J Mol Cell Cardiol.* 2007;42:931-945.
6. Radicke S, Vaquero M, Caballero R, Gómez R, Núñez L, Tamargo J, Ravens U, Wettwer E, Delpón E. Effects of MiRP1 and DPP6 beta-subunits on the blockade induced by flecainide of Kv4.3/KChIP2 channels. *Br J Pharmacol*. 2008;154:774-786.

7. Delpón E, Cordeiro JM, Núñez L, Thomsen PE, Guerchicoff A, Pollevick GD, Wu Y, Kanters JK, Larsen CT, Burashnikov E, Christiansen M, Antzelevitch C. Functional Effects of KCNE3 Mutation and its Role in the Development of Brugada Syndrome. *Circ Arrhythm Electrophysiol.* 2008;1:209-218.
8. Núñez L, Vaquero M, Gómez R, Caballero R, Mateos-Cáceres P, Macaya C, Iriepa I, Gálvez E, López-Farré A, Tamargo J, Delpón E. Nitric oxide blocks hKv1.5 channels by S-nitrosylation and by a cyclic GMP-dependent mechanism. *Cardiovasc Res*. 2006;72:80-89.
9. Piao L, Li J, McLerie M, Lopatin AN. Cardiac I_{K1} underlies early action potential shortening during hypoxia in the mouse heart. *J Mol Cell Cardiol.* 2007;43:27-38.
10. Picones A, Keung E, Timpe LC. Unitary conductance variation in Kir2.1 and in cardiac inward rectifier potassium channels. *Biophys J*. 2001;81:2035-2049.
11. Neher E. Correction for liquid junction potentials in patch clamp experiments. *Methods Enzymol*. 1992;207:123-131.
12. Voigt N, Friedrich A, Bock M, Wettwer E, Christ T, Knaut M, Strasser RH, Ravens U, Dobrev D. Differential phosphorylation-dependent regulation of constitutively active and muscarinic receptor-activated IK,ACh channels in patients with chronic atrial fibrillation. *Cardiovasc Res.* 2007;74:426-437.
13. Ahmmed GU, Xu Y, Hong Dong P, Zhang Z, Eiserich J, Chiamvimonvat N. Nitric oxide modulates cardiac Na^+ channel via protein kinase A and protein kinase G. *Circ Res*. 2001;89:1005-1013.
14. Lizarbe TR, García-Rama C, Tarín C, Saura M, Calvo E, López JA, López-Otín C, Folgueras AR, Lamas S, Zaragoza C. Nitric oxide elicits functional MMP-13 protein-tyrosine nitration during wound repair. *FASEB J.* 2008;22:3207-3215.

Online **Table I.** Patient characteristics

Mean age (y)	72±6
Female (*n*)	8/15
Chronic Atrial Fibrillation	2/15
Surgery	
Valve surgery (*n*)	13/15
CABG surgery (*n*)	8/15
Treatment	
Beta blockers	9/15
ACE inhibitors/angiotensin receptor blockers	13/15
Statins	11/15
Acetylsalicylic acid	9/15

ACE, angiotensin converting enzyme; CABG, coronary artery bypass grafting.